Absorption of high-contrast 12-ps uv laser pulses by solid targets

D. Riley, L. A. Gizzi, A. J. Mackinnon, S. M. Viana, and O. Willi
The Blackett Laboratory, Imperial College of Science, Technology and Medicine, Prince Consort Road, London SW7 2BZ, England
(Received 11 August 1993)

The absorption of 12-ps prepulse free-laser pulses from a Raman amplified KrF laser has been measured at normal incidence for irradiances between 10^{14} and 10^{17} W cm^{-2}, and as a function of incident angle at 5×10^{16} W cm^{-2}, for both P and S polarizations. It is found that the main features of the experimental data are reasonably well modeled by a combination of resonance and collisional absorption, using a semianalytical treatment.

PACS number(s): 52.50.Jm

The current interest in the interaction of short-pulse lasers with solid targets is partly motivated by their application to the generation of bright, short-lived coherent and incoherent sources of x-rays and to their ability to generate hot plasmas at high density [1]. The controlling factor in all such experiments is the level and mechanisms of laser-light absorption, which in experiments to date generally means collisional and resonance absorption [2–5]. This paper reports on an experiment to measure the absorption fraction when a short-pulse laser, which is well suited to both high-density plasma generation and x-ray-laser applications, is focused onto solid targets under varying irradiances, angles of incidence, and laser polarization.

The SPRITE laser at Rutherford Appleton Laboratory produces Raman amplified KrF pulses of 12-ps duration at 268 nm wavelength [6]. The laser has low divergence (2× diffraction limit) and produces up to 6 J of energy (about 3.5 J on target). Although 12 ps is long enough for significant hydrodynamic motion to occur, the high incident irradiances possible (in excess of 10^{17} W cm^{-2}) and short wavelength allow hot plasma to be produced at high density. The amplified spontaneous emission (ASE) prelase of the laser has been shown to be less than 10^{-10} of the main pulse intensity; thus even for the highest irradiances the pulse interacts with a solid surface rather than a preformed plasma.

The laser was directed onto solid aluminum targets with an off-axis paraboloid with approximately $f/4.7$ focusing. The targets were mounted on a translatable rotating stage. The axis of rotation was changed to alternate from P to S polarization. The position of the target was controlled to 10 μm by a high-magnification television alignment system. Because of this, the variation in spot size was kept small. Overall shot-to-shot variation in irradiance, including energy fluctuation, was about 15%. An angled plate was used to direct a portion of the directly backscattered light onto a fluorescent sample that converted the uv light to optical radiation which was detected by a calibrated photodiode. This system was carefully checked to have a linear response for light levels used in the experiment. The light not directly backscattered was collected by an Ulbricht sphere around the target. A small aperture allowed the alignment system to view the target. A further diagnostic hole was used to monitor the x-ray focal spot via a pinhole camera fitted with a 5-μm-diam. pinhole which was filtered with 25 μm beryllium. The area open for target insertion and diagnostics was about 3.6% of the total surface area of the sphere. The scattered energy was measured with a surface absorbing calorimeter. The sphere-calorimeter system was calibrated and tested to be linear for the typical scattered energy densities incident on the sphere surface during the experiment. The scattered light was found to be not quite specular, but largely dispersed into an approximately $f/1.5$ cone, probably due to refraction effects in the focal region, with a maximum of about 15% of incident energy being backscattered in the focusing cone at normal incidence. The targets were solid polished aluminum and were used for several shots by moving the target to expose a fresh surface after each shot.

The experiment was modeled with a semianalytical treatment. We used the formula for collisional absorption in an exponential density ramp in the WKB approximation [6]. The absorption on the way up to the critical density surface is given by reducing the beam intensity by a factor $e^{-\delta}$, where $\delta=4\nu_c L\cos\theta/3c$. L is the scale length, θ is the angle of incidence, and ν_c is the collision frequency evaluated at critical density, where $\nu_{ei}=3\times10^{-6}N_e Z^*\ln\Lambda/T_e^{3/2}$, $\ln\Lambda$ is the Coulomb logarithm, and Z^* is the average degree of ionization. The high field of the laser reduces the effective collision frequency by a factor $(1+v_{\rm osc}^2/v_{\rm th}^2)^{3/2}$, where $v_{\rm osc}$ and $v_{\rm th}$ are the oscillation and thermal electron velocities, respectively. The value of $v_{\rm osc}$ includes the effects of field swelling at the maximum given by $(E/E_0)^2=3.5(2\pi\omega L/c)^{1/3}$ [7]. Resonance absorption was then accounted for using the standard Denisov function [8], which depends on scale length and angle of incidence as well as the laser wavelength. The focusing of the laser results in a residual P component that gives rise to a nontrivial amount of resonance absorption even for S-polarized light. This is accounted for by taking a weighted average over the flat-topped beam profile for $f/4.7$ focusing when calculating the resonance absorption. The nominally S-polarized light at oblique incidence still has an effective P component due to focusing, which is treated as in the normal-incidence case, except that the resonantly absorbed fraction is reduced by a factor of the form

 ©1993 The American Physical Society

$\cos^2\theta e^{-2\beta}$ [where $\beta=(2\omega_I L/3c)\sin^3\theta$, and ω_1 is the laser frequency] and represents the reduction in the E-field component parallel to the density gradient and the extra evanescent decay between the turning point and the critical surface, due to the oblique angle of incidence. Finally, the collisional absorption as the beam leaves the plasma is accounted for by a further reduction in intensity by the factor $e^{-\delta}$.

In order to be self-consistent, the model requires a functional relationship between the scale length, temperature, and absorbed irradiance. This is achieved with a one-dimensional (1D) hydrocode [9] with a varying absorption fraction at critical density, for 12-ps Gaussian uv pulses. The scale length L at critical is calculated by the best fit to a profile of the type $N=N_c e^{-x/L}$. This form was used, as it gave a simple expression that closely represented the simulated profile. The standard resonance absorption theory is, strictly speaking, applicable to a linear profile; however, if the turning point is close to the critical density surface we can apply the theory with the exponential scale length to a reasonable approximation even for moderate angles of incidence. The temperature is taken at about the critical density, as this is the most important region for absorption. At the peak of the pulse, the fits we find are

$$L(\mathrm{m})=4.28\times10^{-11}[I_{\mathrm{abs}}(\mathrm{W\,cm^{-2}})]^{0.306}\ , \quad (1)$$

$$T(\mathrm{eV})=9.05\times10^{-7}[I_{\mathrm{abs}}(\mathrm{W\,cm^{-2}})]^{0.615}\ . \quad (2)$$

After assuming an initial value for absorption, Newton-Raphson iteration is then used to calculate self-consistent values of the absorption, scale length, and temperature.

Figure 1 shows the measured absorption for normal incidence as a function of irradiance. Up to about 10^{16} W cm^{-2}, the main absorption mechanism is predicted to be inverse bremsstrahlung. Beyond this point, resonance absorption becomes the dominant mechanism. At high irradiance, the semianalytical model seems to work quite well, but is not so good at lower irradiance. However, we note that for the low-irradiance data the scale length is predicted to be of the order of 1 μm, which is only a few times the laser wavelength, and thus the collisional absorption model which is derived in the WKB approximation may not work so well under these conditions.

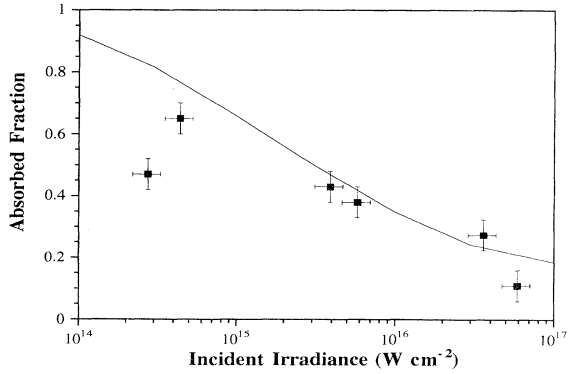

FIG. 1. Experimental absorption as a function of incident irradiance for normal incidence. The solid line is the prediction of the model. The vertical error bars are derived from the calibration data. Horizontal error bars are based on positioning accuracy of the alignment system.

Figure 2 shows the reflected fraction as a function of angle of incidence for P- and S- polarized light. All shots are close to an irradiance of 5×10^{16} W cm^{-2}. The solid lines refer to the analytical model. For P polarization, considering that the peak angle is not assumed *a priori*, the agreement with experiment is very satisfactory. Standard resonance absorption theory predicts that, for 0.268-μm light, the scale length associated with a peak at 10° corresponds to a scale length of around 4 μm. This means that L/λ is greater than 10, justifying the WKB approximation in this case. Also, the hydrodynamic simulations show that the critical surface moves out only 2.5μm during the pulse, which justifies to a reasonable level the 1D approximation for these data which were taken with a 20-μm focal spot.

For S polarization the model predictions fall off with angle in the right way but there seems to be a systematic disagreement of a few percent of incident energy. Several explanations were considered and rejected; no obvious experimental difference could be responsible, as the target rather than the laser is reoriented to change the effective polarization, so optical components should behave in the same manner. The model predicts that at normal incidence only 9% of incident laser energy is absorbed by inverse bremsstrahlung, so that the explanation would seem to lie with the modeling of resonance absorption.

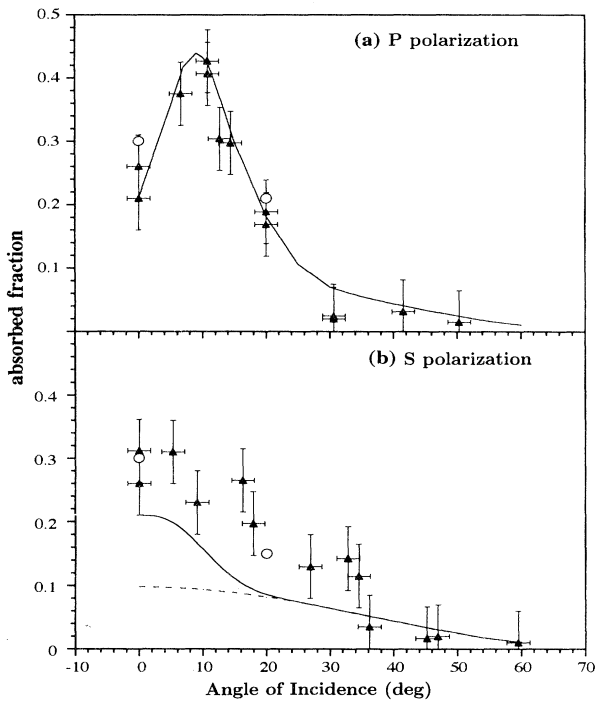

FIG. 2. Absorption vs angle of incidence for (a) P polarization and (b) S polarization. The solid line is the model prediction; the broken line in (b) is a calculation with only collisional absorption. The open circles represent the simulation results described in the text. The error bars in angle represent the angular steps (1.8°) in the target mount rotation.

Rippling of the target surface would enhance absorption by increasing the spread of angles over which the resonance absorption is averaged; however, the well defined peak for P-polarized light and good agreement for peak absorption fraction suggest this is not a major effect, and indeed by artificially increasing the range of angles included we were not able to resolve the discrepancy for S polarization without losing the agreement for P polarization.

In our view, the most likely explanation of the disagreement with the data relates to the use of a single scale length, i.e., at the peak of the pulse. Later in the pulse, the scale length becomes longer, and if the effective resonance absorption angle of incidence is less than the peak angle (10° in our case) then we expect an enhancement of resonance absorption late in time. This will be true for all the S-polarized shots. In the P-polarized case we expect some enhancement at low angles and a slight shift in the peak. Hydrodynamic simulations suggest that this shift would only be of the order 1°.

The open circles in Fig. 2 represent hydrodynamic simulations in which a similar resonance absorption model to that described above is used. The collisional absorption takes place in all cells up to critical density, with high-field corrections applied as described above. The laser light refraction is approximated by using Snell's law at cell interfaces, with a minimum refractive index near critical density given by the same wavelength-averaging arguments that Kruer [7] uses to reproduce the correct field-swelling limit. We limit ourselves to lower angles and few runs because producing a fine enough cell zoning presents a problem at too oblique an angle, and the simulations become expensive in computer time. However, for 0° and 20° we can see that the effect is largest for S polarization and the results are closer to experiment, without losing the good agreement with the P-polarized case.

The model we have used has several approximations that should be discussed further. The assumption of planarity was justified by comparing the distance moved by the critical surface and the focal spot width. For the higher-irradiance case the underdense plasma should extend several micrometers, and thus will not be completely planar away from the critical surface. This could help explain why, at high irradiance, the scattered light was found to be not quite specular, but largely dispersed into an approximately $f/1.5$ cone, with a maximum of about 15% of incident energy being backscattered in the focusing cone at normal incidence. This would result in a cooler plasma in the corona than predicted by the 1D model. On the other hand, this would not enhance collisional absorption very much, as the high-field effects are very strong. The effect of parametric instabilities has not been considered. For the conditions of temperature and scale length in Fig. 2, the irradiance is below the threshold for Raman backscatter and the two-plasmon decay instability. However, it is close to the threshold for stimulated Brillouin backscatter (SBS) and indeed about 4% backscatter at incident angles greater than 30° was found, which could be attributed to SBS. The laser intensity is above the collisional threshold for exciting the oscillating two-stream instability close to critical density, and the ion acoustic decay instability in the region above around 0.8 times the critical density. However, given that the region for gain is very small (less than 1μm, depending on the details of the profile close to critical density), we estimate that, in both cases, the convective loss rate due to the steep gradient will prevent significant growth. Unfortunately, we were unable to monitor the second harmonic emission spectrum for a Stokes sideband related to the ion acoustic decay as, for our laser, it occurs in an experimentally difficult wavelength range.

Another effect neglected is the generation of a large magnetic field by the $\nabla N \times \nabla T$ mechanism [10]. By taking the usual theory [11] and considering the density gradient inferred, the temperature predicted, and the focal spot size, we can estimate that fields of the order 10 MG may be generated. However, the magnetic field pressure is then of the order 4 Mbar, compared to over 100 Mbar at critical density for the predicted temperature, so no major hydrodynamic modification seems likely. Kruer and Estabrook [12] have predicted that the $\mathbf{v} \times \mathbf{B}$ force from electrons oscillating in the laser electric field normal to a B field may drive plasma waves which then absorb energy as they are damped. This would affect both polarizations and does not appear to be needed as an extra absorption mechanism. We note that the B field is weakest at the center of the focal spot where most laser energy is incident, and $\mathbf{v}_{\rm osc} \times \mathbf{B}$ may be small compared to the electric field driving conventional resonance absorption, E_d.

Finally, we find that the most serious omission is the ponderomotive steepening that should occur at the critical density surface. For the data in Fig. 2 at normal incidence, we have approximately $v_{\rm osc}/v_{\rm th} = 0.2$, where $v_{\rm osc}$ is the oscillation velocity in the vacuum electric field. This ought to have a significant effect on the scale length of the plasma near critical density, resulting in a shift of the absorption peak to a higher angle. In fact the peak angle in the model agrees well with experiment without including the profile steepening. Why this should be so is not yet clear. We note, however, that the peak angle scales weakly with scale length [$\sin\theta \sim L^{-1/3}$], so that a shift in the peak of only 2° corresponds to a 70% reduction in scale length to around 2.3 μm. This would alter the details of the collisional absorption and more importantly the residual resonance absorption at normal incidence. To include the ponderomotive force properly in the analysis would require a more sophisticated model than we have available at present. The residual resonance absorption due to focusing, possible 2D expansion in the coronal plasma, and, possibly, large B-field generation would have to be accounted for in such a model, which would be computationally expensive.

In conclusion we have measured the absorption of high-contrast short uv laser pulses at high irradiance. The behavior with irradiance and angle is consistent with a combination of inverse bremsstrahlung and resonance absorption. We predict that for nominally S-polarized light at high irradiance, the residual resonance absorption due to focusing geometry can be more important than collisional absorption. The role of profile steepening

warrants further investigation with a more sophicated model. However, as a first iteration our simple model is very fast and yields relatively good results that show up the essential features of the experimental data.

We would like to thank the SPRITE laser staff of the Rutherford-Appleton Laboratory Central Laser Facility for their cooperation in carrying out the experiments. This work was jointly funded by an SERC/MoD grant.

[1] D. Riley, L. A. Gizzi, F. Y. Khattak, A. J. MacKinnon, S. M. Viana, and O. Willi, Phys. Rev. Lett. **69**, 3739 (1992).
[2] J. C. Kieffer, P. Audebert, M. Chaker, J. P. Matte, H. Pépin, T. W. Johnston, P. Maine, D. Meyerhofer, J. Delettrez, D. Strickland, P. Bado, and G. Mouro, Phys. Rev. Lett. **62**, 760 (1989).
[3] R. Fedosejevs, R. Ottman, R. Sigel, G. Kühnle, S. Szatmari, and F. P. Schäfer, Phys. Rev. Lett. **64**, 1250 (1990).
[4] R. P. Godwin, R. Sachsenmaier, and R. Sigel, Phys. Rev. Lett. **39**, 1198 (1977).
[5] K. R. Manes, V. C. Rupert, J. M. Auerbach, P. Lee, and J. E. Swain, Phys. Rev. Lett. **39**, 281 (1977).
[6] E. C. Harvey *et al.*, Rutherford-Appleton Laboratory Report No. RAL-91-025, 1991 (unpublished), p. 77.
[7] W. L. Kruer, *The Physics of Laser Plasma Interactions* (Addison-Wesley, Reading, MA, 1988).
[8] G. J. Pert, Plasma Phys. **20**, 175 (1978).
[9] J. P. Christiansen, D.E.T.F. Ashby, and K. V. Roberts, Comput. Phys. Commun. **7**, 271 (1974).
[10] J. A. Stamper and B. H. Ripin, Phys. Rev. Lett. **34**, 138 (1975).
[11] C. E. Max, Lawrence Livermore National Laboratory Report No. UCRL-53107, 1981 (unpublished).
[12] W. L. Kruer and K. Estabrook, Phys. Fluids **20**, 1688 (1977).